critical for future clinical trials to provide improved assignment of treatment intensity and greater insight into the role of biologic and clinical tumor features on patient survival.

In conclusion, although the INSS stage 4S metastatic pattern has a more favorable outcome than stage 4 pattern in the age group of 0 to 18 months, biologic categorization of risk, particularly by *MYCN*, MKI, 11q, 1p, and histology, is more critical than metastatic pattern to assign risk-adapted therapy. In addition, infants in the very young age group (ie, age younger than 19 days) may require different management.

AUTHORS' DISCLOSURES OF POTENTIAL CONFLICTS OF INTEREST

The author(s) indicated no potential conflicts of interest.

AUTHOR CONTRIBUTIONS

Conception and design: Denah R. Taggart, Wendy B. London, Mary Lou Schmidt, Katherine K. Matthay
Financial support: Wendy B. London
Provision of study materials or patients: Tom F. Monclair, Akira Nakagawara, Bruno De Bernardi, Susan L. Cohn, Katherine K. Matthay
Collection and assembly of data: Wendy B. London, Tom F. Monclair, Akira Nakagawara, Bruno De Bernardi, Peter F. Ambros, Andrew D.J. Pearson, Susan L. Cohn, Katherine K. Matthay
Data analysis and interpretation: Denah R. Taggart, Wendy B. London, Mary Lou Schmidt, Steven G. DuBois, Peter F. Ambros, Susan L. Cohn, Katherine K. Matthay
Manuscript writing: All authors
Final approval of manuscript: All authors

REFERENCES

1. D'Angio G, Evans A, Koop C: Special pattern of widespread neuroblastoma with a favourable prognosis. Lancet 1:1046-1049, 1971
2. Brodeur GM, Pritchard J, Berthold F, et al: Revisions of the international criteria for neuroblastoma diagnosis, staging, and response to treatment. J Clin Oncol 11:1466-1477, 1993
3. Schleiermacher G, Rubie H, Hartmann O, et al: Treatment of stage 4s neuroblastoma: Report of 10 years' experience of the French Society of Paediatric Oncology (SFOP). Br J Cancer 89:470-476, 2003
4. Nickerson HJ, Matthay KK, Seeger RC, et al: Favorable biology and outcome of stage IV-S neuroblastoma with supportive care or minimal therapy: A Children's Cancer Group study. J Clin Oncol 18:477-486, 2000
5. Bourhis J, Dominici C, McDowell H, et al: N-myc genomic content and DNA ploidy in stage IVS neuroblastoma. J Clin Oncol 9:1371-1375, 1991
6. DuBois SG, Kalika Y, Lukens JN, et al: Metastatic sites in stage IV and IVS neuroblastoma correlate with age, tumor biology, and survival. J Pediatr Hematol Oncol 21:181-189, 1999
7. Hachitanda Y, Hata J: Stage IVS neuroblastoma: A clinical, histological, and biological analysis of 45 cases. Hum Pathol 27:1135-1138, 1996
8. Wang Q, Diskin S, Rappaport E, et al: Integrative genomics identifies distinct molecular classes of neuroblastoma and shows that multiple genes are targeted by regional alterations in DNA copy number. Cancer Res 66:6050-6062, 2006
9. Katzenstein HM, Bowman LC, Brodeur GM, et al: Prognostic significance of age, MYCN oncogene amplification, tumor cell ploidy, and histology in 110 infants with stage D S neuroblastoma: The pediatric oncology group experience—A pediatric oncology group study. J Clin Oncol 16:2007-2017, 1998
10. Guo C, White PS, Weiss MJ, et al: Allelic deletion at 11q23 is common in MYCN single copy neuroblastomas. Oncogene 18:4948-4957, 1999
11. Maris JM, Hogarty MD, Bagatell R, et al: Neuroblastoma. Lancet 369:2106-2120, 2007
12. Maris JM, Matthay KK: Molecular biology of neuroblastoma. J Clin Oncol 17:2264-2279, 1999
13. van Noesel MM, Heahlen K, Hakvoort-Cammel FG, et al: Neuroblastoma 4S: A heterogeneous disease with variable risk factors and treatment strategies. Cancer 80:834-843, 1997
14. Schneiderman J, London WB, Brodeur GM, et al: Clinical significance of MYCN amplification and ploidy in favorable-stage neuroblastoma: A report from the Children's Oncology Group. J Clin Oncol 26:913-918, 2008
15. George RE, London WB, Cohn SL, et al: Hyperdiploidy plus nonamplified MYCN confers a favorable prognosis in children 12 to 18 months old with disseminated neuroblastoma: A Pediatric Oncology Group study. J Clin Oncol 23:6466-6473, 2005
16. Schmidt ML, Lal A, Seeger RC, et al: Favorable prognosis for patients 12 to 18 months of age with stage 4 nonamplified MYCN neuroblastoma: A Children's Cancer Group Stuoy. J Clin Oncol 23: 6474-6480, 2005
17. Monclair T, Brodeur GM, Ambros PF, et al: The International Neuroblastoma Risk Group (INRG) staging system: An INRG Task Force report. J Clin Oncol 27:298-303, 2009
18. Shimada H, Ambros IM, Dehner LP, et al: The International Neuroblastoma Pathology Classification (the Shimada system). Cancer 86:364-372, 1999
19. Bagatell R, Beck-Popovic M, London WB, et al: Significance of MYCN amplification in international neuroblastoma staging system stage 1 and 2 neuroblastoma: A report from the International Neuroblastoma Risk Group database. J Clin Oncol 27: 365-370, 2009
20. Ambros PF, Ambros IM, Brodeur GM, et al: International consensus for neuroblastoma molecular diagnostics: Report from the International Neuroblastoma Risk Group (INRG) Biology Committee. Br J Cancer 100:1471-1482, 2009
21. Cohn SL, Pearson AD, London WB, et al: The International Neuroblastoma Risk Group (INRG) classification system: An INRG Task Force report. J Clin Oncol 27:289-297, 2009
22. Kaplan EL, Meier P: Nonparametric estimation from incomplete observations. J Am Stat Assoc 53:457-481, 1958
23. Peto R, Pike MC, Armitage P, et al: Design and analysis of randomized clinical trials requiring prolonged observation of each patient: I. Introduction and design. Br J Cancer 34:585-612, 1976
24. Cox DR: Regression models and life tables. J R Stat Soc B 34:187-220, 1972
25. Segal MR: Extending the elements of tree-structured regression. Stat Methods Med Res 4: 219-236, 1995
26. Segal MR, Bloch DA: A comparison of estimated proportional hazards models and regression trees. Stat Med 8:539-550, 1989
27. London WB, Castleberry RP, Matthay KK, et al: Evidence for an age cutoff greater than 365 days for neuroblastoma risk group stratification in the Children's Oncology Group. J Clin Oncol 23:6459-6465, 2005
28. Schmidt ML, Lukens JN, Seeger RC, et al: Biologic factors determine prognosis in infants with stage IV neuroblastoma: A prospective Children's Cancer Group study. J Clin Oncol 18:1260-1268, 2000
29. De Bernardi B, Gerrard M, Boni L, et al: Excellent outcome with reduced treatment for infants with disseminated neuroblastoma without *MYCN* gene amplification. J Clin Oncol 27:1034-1040, 2009
30. Canete A, Gerrard M, Rubie H, et al: Poor survival for infants with *MYCN*-amplified metastatic neuroblastoma despite intensified treatment: The International Society of Paediatric Oncology European neuroblastoma experience. J Clin Oncol 27: 1014-1019, 2009
31. Baker DL, Schmidt ML, Cohn SL, et al: Outcome after reduced chemotherapy for intermediate-risk neuroblastoma. N Engl J Med 363:1313-1323, 2010
32. Attiyeh EF, London WB, Mosse YP, et al: Chromosome 1p and 11q deletions and outcome in neuroblastoma. N Engl J Med 353:2243-2253, 2005
33. Spitz R, Hero B, Simon T, et al: Loss in chromosome 11q identifies tumors with increased risk for metastatic relapses in localized and 4S neuroblastoma. Clin Cancer Res 12:3368-3373, 2006

Clinical Cancer Research

Expression of *NLRR3* Orphan Receptor Gene Is Negatively Regulated by MYCN and Miz-1, and Its Downregulation Is Associated with Unfavorable Outcome in Neuroblastoma

Jesmin Akter[1,2], Atsushi Takatori[1], Md. Shamim Hossain[1], Toshinori Ozaki[1,3], Atsuko Nakazawa[5], Miki Ohira[4], Yusuke Suenaga[1], and Akira Nakagawara[1,2]

Abstract

Purpose: Our previous study showed that expression of NLRR3 is significantly high in favorable neuroblastomas (NBL), whereas that of NLRR1 is significantly high in unfavorable NBLs. However, the molecular mechanism of transcriptional regulation of *NLRR3* remains elusive. This study was undertaken to clarify the transcriptional regulation of *NLRR3* and its association with the prognosis of NBL.

Experimental Design: *NLRR3* and *MYCN* expressions in NBL cell lines were analyzed after induction of cell differentiation, MYCN knockdown, and overexpression. The transcriptional regulation of *NLRR3* was analyzed by luciferase reporter and chromatin immunoprecipitation assays. Quantitative PCR was used for examining the expression of *NLRR3*, *Miz-1*, or *MYCN* in 87 primary NBLs.

Results: The expression of *NLRR3* mRNA was upregulated during differentiation of NBL cells induced by retinoic acid, accompanied with reduced expression of *MYCN*, suggesting that *NLRR3* expression was inversely correlated with *MYCN* in differentiation. Indeed, knockdown of *MYCN* induced *NLRR3* expression, whereas exogenously expressed MYCN reduced cellular *NLRR3* expression. We found that Miz-1 was highly expressed in favorable NBLs and *NLRR3* was induced by *Miz-1* expression in NBL cells. MYCN and Miz-1 complexes bound to *NLRR3* promoter and showed a negative regulation of *NLRR3* expression. In addition, a combination of low expression of *NLRR3* and high expression of *MYCN* was highly associated with poor prognosis.

Conclusions: *NLRR3* is a direct target of MYCN, which associates with Miz-1 and negatively regulates *NLRR3* expression. NLRR3 may play a role in NBL differentiation and the survival of NBL patients by inversely correlating with *MYCN* amplification. *Clin Cancer Res; 17(21); 6681–92. ©2011 AACR.*

Introduction

Neuroblastoma (NBL) is one of the most common malignant solid tumors in children and accounts for 8% of all pediatric cancers (1). NBLs originate from sympathetic precursor neuroblasts derived from the neural crest. NBLs found in patients older than 1 year are usually aggressive and eventually kill the patients despite intensive therapy, whereas those in patients younger than 1 year often regress spontaneously or maturate, resulting in a favorable prognosis (2). We have made extensive efforts to show that TrkA, a high-affinity receptor for nerve growth factor, and TrkB, a receptor for brain-derived neurotrophic factor as well as neurotrophin 4/5, are important key regulators (3–6). However, the precise molecular mechanisms of how NBL becomes aggressive and how the spontaneous regression is induced still remain elusive.

Amplification of the *MYCN* oncogene is strongly associated with rapid progression of NBL (7). The *MYCN* amplification occurs in approximately 25% of NBL and is one of the most important prognostic indicators of poor clinical outcome (8–12). MYCN is a nuclear transcription factor and its expression level is well associated with cell proliferation of NBL cells (13, 14). In general, MYCN exerts its biological functions through transcriptional regulation of its target genes in both positive and negative manners. MYCN has an ability to activate its target genes by forming a heterodimer with MAX and binds to the E-box motif, CACGTG, in the proximal promoter region (15–18). On the contrary, MYCN represses the expression of genes, such

Authors' Affiliations: [1]Division of Biochemistry and Innovative Cancer Therapeutics, Chiba Cancer Center; [2]Department of Molecular Biology and Oncology, Chiba University Graduate School of Medicine; [3]Laboratories of Anti-Tumor Research and [4]Cancer Genomics, Chiba Cancer Center Research Institute, Chiba; and [5]Department of Pathology, National Center for Child Health and Development, Tokyo, Japan

Note: Supplementary data for this article are available at Clinical Cancer Research Online (http://clincancerres.aacrjournals.org/).

Corresponding Author: Akira Nakagawara, Division of Biochemistry and Innovative Cancer Therapeutics, Chiba Cancer Center, 666-2 Nitona, Chuoh-ku, Chiba 260-8717, Japan. Phone: 81-43-264-5431; Fax: 81-43-265-4459; E-mail: akiranak@chiba-cc.jp

doi: 10.1158/1078-0432.CCR-11-0313

Translational Relevance

Amplification of *MYCN* oncogene is strongly associated with rapid progression of neuroblastoma (NBL) and one of the most important prognostic indicators of poor clinical outcome. Our group previously reported that NLRR3 is highly expressed in a favorable subset of NBL but until this work, there was no sound investigation of the function of NLRR3 and its transcriptional regulation. In this study, we found that *NLRR3* is a direct target of MYCN but its expression is negatively regulated by MYCN in association with Miz-1. Furthermore, a combination of low expression level of *NLRR3* and high expression level of *MYCN* was strongly correlated with the poor prognosis. These data suggest that the expression pattern of NLRR3, Miz-1, and MYCN plays an important role in defining the clinical behavior of NBLs. The decreased expression of NLRR3 might be one of the key events regulating the aggressive behavior of NBL.

as $p15^{INK4b}$, $p21^{CIP1}$, and *NDRG2*, when it forms a complex with transcriptional regulators, such as Myc-interacting zinc finger protein 1 (Miz-1) and Sp1 (19–21). Koppen and colleagues have previously described that MYCN suppresses *Dickkopf-1* (*DKK1*) expression, resulting in proliferation of NBL cells (22). However, the precise mechanism of how MYCN contributes to NBL aggressiveness remains unclear.

We have identified human neuronal leucine-rich repeat (NLRR) family genes as one of the differentially expressed genes between favorable and unfavorable NBLs, using our unique NBL cDNA libraries (23, 24). The NLRR protein family consists of 3 members, NLRR1, NLRR2, and NLRR3 (23), and belongs to the type *y* transmembrane protein with leucine-rich repeat (LRR) domains containing 11 or 12 LRRs, an immunoglobulin c2-type domain, and a fibronectin type III domain in its extracellular region. The amino acid sequences of NLRR family proteins are highly conserved in the extracellular domains, and NLRR1 and NLRR3 also possess a conserved stretch of 11 amino acids with 2 clathrin adapter interaction domains and a dileucine-type domain in the short intracellular region (25, 26), which might provide a basis for NLRR function. Our previous reports showed that NLRR1 is a direct transcriptional target of MYCN and that a high expression level of *NLRR1* mRNA is associated with a poor prognosis of NBL (23, 27). However, the function of NLRR3 is poorly understood except that mouse *NLRR3* expression is increased in the cerebral cortex after a cortical brain injury (28) and that rat NLRR3 may be involved in the regulation of EGF receptor signaling through interaction with clathrins (26).

We have previously reported that high levels of *NLRR3* mRNA expression are associated with favorable prognostic factors in NBL (23). In this study, we found that NLRR3 is induced during differentiation of NBL cells. Transcriptional analysis has revealed that NLRR3 is a direct transcriptional target of MYCN, which negatively transactivates it in association with Miz-1. Furthermore, high expression of *NLRR3* or *Miz-1* and the combination of high expression of both *NLRR3* and *Miz-1* are significantly associated with a favorable outcome of NBL. On the contrary, the low expression levels of *NLRR3* and high expression of *MYCN* were strongly correlated with a poor prognosis of NBL.

Materials and Methods

Patient population

Eighty-seven patients with NBL were diagnosed clinically and histologically, using a surgically removed tumor specimen according to the International Neuroblastoma Pathological classification (INPC). According to the International NBL Staging System (INSS; ref. 29), 18 patients were diagnosed as stage 1, 11 were stage 2, 20 were stage 3, 33 were stage 4, and 5 were stage 4S. Cytogenetic and molecular biological analysis of all tumors was also carried out by assessing DNA ploidy, *MYCN* amplification, and *TrkA* expression. The patients were then treated following the protocols proposed by the Japanese Infantile NBL Cooperative Study (30) and Group for Treatment of Advanced NBL (31), and subjected to survival analysis of the result in a follow-up period of at least 36 months (range, 4–58). The study was conducted under internal review board approval with appropriate informed consent.

Cell lines and transient transfection

Human NBL-derived cell lines, including SK-N-BE, CHP134, IMR32, GOTO, KAN, KP-N-NS, LAN-5, NB-1, NB-9, NLF, RTBM1, SK-N-DZ, TGW, NB69, NBL-S, OAN, SK-N-AS, SK-N-SH, and SH-SY5Y cells were obtained from the CHOP cell line bank (Philadelphia, PA) and maintained in a culture condition, using RPMI 1640 supplemented with 10% heat-inactivated FBS (Invitrogen), 100 IU/mL penicillin, and 100 μg/mL streptomycin in a 37°C, 5% CO_2 incubator. For the NBL cell differentiation experiment, RTBM1 and SH-SY5Y cells were exposed to all-*trans* retinoic acid (ATRA; Sigma) at a final concentration of 5 μmol/L. For transient transfection, cells were transfected with the indicated expression of plasmids by using a Lipofectamine 2000 transfection reagent (Invitrogen), according to the manufacturer's recommendations.

RNA extraction and semiquantitative reverse transcriptase PCR

Total RNA was prepared from fresh-frozen tissues of primary NBLs or cultured cells by using Trizol reagents (Life Technologies) or the RNeasy Mini kit (Qiagen). Reverse transcription was carried out by random primers and Superscript II (Invitrogen), following the manufacturer's instructions. After reverse transcription, the resultant cDNA was subjected to PCR-based amplification. The sequence of the primer sets were used for PCR amplification is listed in the Supplementary Table S4. All PCR amplifications were carried out with a GeneAmp PCR 9700 (Perkin-Elmer Co), using rTaq DNA polymerase (Takara).

The expression of *GAPDH* was measured as an internal control.

Quantitative real-time PCR

cDNA from primary NBLs and cell lines were subjected to the real-time PCR to quantitate the expression levels of *MYCN*, *Miz-1*, and *NLRR3* mRNA. TaqMan GAPDH control reagent kit (Perkin-Elmer Applied Biosystems) was used for *GAPDH* expression and analyzed by an ABI prism 7500 Sequence Detection System (Applied Biosystems). *NLRR3* and *Miz-1* TaqMan probes were purchased from Applied Biosystems. *MYCN* mRNA expression was measured by the SYBR green real-time PCR system. The primers and probes used for real-time PCR were listed in Supplementary Table S4.

Generation of a specific antibody against NLRR3

The rabbit polyclonal anti-NLRR3 antibody was raised against a mixed synthetic peptide corresponding to amino acid sequences between positions 655 to 670 and 692 to 707 of human NLRR3. The peptide and polyclonal antibody (TB0266) were generated by Medical and Biological Laboratories (Nagoya, Japan). The specificity of the affinity-purified antibody was assayed by immunoblotting.

Plasmid constructs

The protein-coding region of *Miz-1* was amplified by PCR and inserted into the *Eco*RI site of pcDNA3.1 (Invitrogen) flanked with a Flag tag. The human *NLRR3* promoter region and its 5′ progressive deletion mutant were amplified by PCR and then inserted into the *Sacy* site in the upstream of the luciferase gene of the pGL3-basic plasmid (Promega). All constructs were verified by DNA sequencing. The pUHD-MYCN vector was kindly provided by Dr. M. Schwab (German Cancer Research Center, Heidelberg, Germany).

Luciferase reporter assay

SH-SY5Y cells were seeded at a density of 5×10^4 cells/12-well cell culture plate and allowed to attach overnight. The cells were transiently cotransfected with each mutant of the human *NLRR3* promoter-driven luciferase reporter and an internal control vector for *Renilla* luciferase, or a combination of the indicated expression vectors. The total amount of plasmid DNA per transfection was kept consistent with the pcDNA3.1 vector. Both firefly and *Renilla* luciferase activities were assayed with the Dual-Luciferase reporter assay system (Promega) according to the manufacturer's instructions. The firefly luminescence signal was normalized on the basis of the *Renilla* luminescence signal.

siRNA transfection

To knockdown endogenous MYCN expression, SK-N-AS, SK-N-BE, and SH-SY5Y cells were transfected with 10 nmol/L of the indicated siRNA purchased from Dharmacon by using LipofectAMINE RNAiMAX (Invitrogen), according to the manufacturer's recommendations. The list of siRNA sequences used will be provided upon request. Forty-eight hours after transfection, cell lysates were prepared and analyzed for the expression levels of NLRR3 and MYCN by immunoblotting.

Immunoblot analysis

The cells were washed twice with ice-cold PBS and then lysed immediately with SDS sample buffer containing 10% glycerol, 5% β-mercaptoethanol, 2.3% SDS, and 62.5 mmol/L Tris-HCl (pH 6.8). The protein concentrations were determined by using Bio-Rad protein assay dye reagent (Bio-Rad Laboratories). Equal amounts of cell lysates were separated by SDS-PAGE and electrophoretically transferred onto Immobilon-P membranes (Millipore). The transferred membranes were blocked with 5% nonfat dry milk in TBS containing 0.1% Tween-20 and incubated with appropriate primary antibodies at room temperature for 1 hour followed by incubation with horseradish peroxidase–conjugated goat anti-mouse or anti-rabbit secondary antibodies (Cell Signaling Technology Inc.) at room temperature for 1 hour. Immunoreactive bands were visualized by an ECL system (GE Healthcare). The primary antibodies used in this study were as follows: monoclonal anti-MYCN (Ab-1; Oncogene Research Products), polyclonal anti-NLRR3, polyclonal anti–Miz-1 (Santa Cruz Biotechnology), monoclonal anti-GAP43 (9-1E21; Chemicon), and polyclonal anti-actin (20-33; Sigma) antibodies.

Chromatin immunoprecipitation assays

A chromatin immunoprecipitation (ChIP) assay was carried out according to the protocol provided by Upstate Biotechnology (Charlottesville). In brief, cells were cross-linked with 1% formaldehyde in medium for 10 minutes at 37°C. Chromatin solutions were prepared and immunoprecipitated with the following antibodies: anti-MYCN, anti–Miz-1, anti-Max rabbit polyclonal antibodies (Santa Cruz Biotechnology), and normal mouse or rabbit serum as a control. The immunoprecipitates were eluted with 100 μL of elution buffer (1% SDS and 1 mmol/L $NaHCO_3$). Formaldehyde-mediated cross-links were reversed by heating at 65°C for 4 hours, and the reaction mixtures were treated with proteinase K at 45°C for 1 hour. DNAs of the immunoprecipitates and control input DNAs were purified by using a QIAquick PCR purification kit (Qiagen). Purified DNA was subjected to optimized semiquantitative PCR amplification protocol for NLRR3 gene promoter and control regions, using appropriate primer sets (Supplementary Table S4).

Statistical analysis

Student *t* tests were employed to examine the possible association between *NLRR3* expression and other prognostic factors. The classification of high and low levels of *NLRR3*, *Miz-1*, and *MYCN* expression was determined on the basis of the mean value obtained from quantitative real-time PCR analysis. Kaplan–Meier survival curves were calculated, and survival distributions were compared by using the log-rank test. Cox regression models were used to search associations along with *NLRR3* expression, *MYCN*

The expression of *GAPDH* was measured as an internal control.

Quantitative real-time PCR

cDNA from primary NBLs and cell lines were subjected to the real-time PCR to quantitate the expression levels of *MYCN*, *Miz-1*, and *NLRR3* mRNA. TaqMan GAPDH control reagent kit (Perkin-Elmer Applied Biosystems) was used for *GAPDH* expression and analyzed by an ABI prism 7500 Sequence Detection System (Applied Biosystems). *NLRR3* and *Miz-1* TaqMan probes were purchased from Applied Biosystems. *MYCN* mRNA expression was measured by the SYBR green real-time PCR system. The primers and probes used for real-time PCR were listed in Supplementary Table S4.

Generation of a specific antibody against NLRR3

The rabbit polyclonal anti-NLRR3 antibody was raised against a mixed synthetic peptide corresponding to amino acid sequences between positions 655 to 670 and 692 to 707 of human NLRR3. The peptide and polyclonal antibody (TB0266) were generated by Medical and Biological Laboratories (Nagoya, Japan). The specificity of the affinity-purified antibody was assayed by immunoblotting.

Plasmid constructs

The protein-coding region of *Miz-1* was amplified by PCR and inserted into the *Eco*RI site of pcDNA3.1 (Invitrogen) flanked with a Flag tag. The human *NLRR3* promoter region and its 5′ progressive deletion mutant were amplified by PCR and then inserted into the *Sacy* site in the upstream of the luciferase gene of the pGL3-basic plasmid (Promega). All constructs were verified by DNA sequencing. The pUHD-MYCN vector was kindly provided by Dr. M. Schwab (German Cancer Research Center, Heidelberg, Germany).

Luciferase reporter assay

SH-SY5Y cells were seeded at a density of 5×10^4 cells/12-well cell culture plate and allowed to attach overnight. The cells were transiently cotransfected with each mutant of the human *NLRR3* promoter-driven luciferase reporter and an internal control vector for *Renilla* luciferase, or a combination of the indicated expression vectors. The total amount of plasmid DNA per transfection was kept consistent with the pcDNA3.1 vector. Both firefly and *Renilla* luciferase activities were assayed with the Dual-Luciferase reporter assay system (Promega) according to the manufacturer's instructions. The firefly luminescence signal was normalized on the basis of the *Renilla* luminescence signal.

siRNA transfection

To knockdown endogenous MYCN expression, SK-N-AS, SK-N-BE, and SH-SY5Y cells were transfected with 10 nmol/L of the indicated siRNA purchased from Dharmacon by using LipofectAMINE RNAiMAX (Invitrogen), according to the manufacturer's recommendations. The list of siRNA sequences used will be provided upon request. Forty-eight hours after transfection, cell lysates were prepared and analyzed for the expression levels of NLRR3 and MYCN by immunoblotting.

Immunoblot analysis

The cells were washed twice with ice-cold PBS and then lysed immediately with SDS sample buffer containing 10% glycerol, 5% β-mercaptoethanol, 2.3% SDS, and 62.5 mmol/L Tris-HCl (pH 6.8). The protein concentrations were determined by using Bio-Rad protein assay dye reagent (Bio-Rad Laboratories). Equal amounts of cell lysates were separated by SDS-PAGE and electrophoretically transferred onto Immobilon-P membranes (Millipore). The transferred membranes were blocked with 5% nonfat dry milk in TBS containing 0.1% Tween-20 and incubated with appropriate primary antibodies at room temperature for 1 hour followed by incubation with horseradish peroxidase–conjugated goat anti-mouse or anti-rabbit secondary antibodies (Cell Signaling Technology Inc.) at room temperature for 1 hour. Immunoreactive bands were visualized by an ECL system (GE Healthcare). The primary antibodies used in this study were as follows: monoclonal anti-MYCN (Ab-1; Oncogene Research Products), polyclonal anti-NLRR3, polyclonal anti–Miz-1 (Santa Cruz Biotechnology), monoclonal anti-GAP43 (9-1E21; Chemicon), and polyclonal anti-actin (20-33; Sigma) antibodies.

Chromatin immunoprecipitation assays

A chromatin immunoprecipitation (ChIP) assay was carried out according to the protocol provided by Upstate Biotechnology (Charlottesville). In brief, cells were cross-linked with 1% formaldehyde in medium for 10 minutes at 37°C. Chromatin solutions were prepared and immunoprecipitated with the following antibodies: anti-MYCN, anti–Miz-1, anti-Max rabbit polyclonal antibodies (Santa Cruz Biotechnology), and normal mouse or rabbit serum as a control. The immunoprecipitates were eluted with 100 μL of elution buffer (1% SDS and 1 mmol/L $NaHCO_3$). Formaldehyde-mediated cross-links were reversed by heating at 65°C for 4 hours, and the reaction mixtures were treated with proteinase K at 45°C for 1 hour. DNAs of the immunoprecipitates and control input DNAs were purified by using a QIAquick PCR purification kit (Qiagen). Purified DNA was subjected to optimized semiquantitative PCR amplification protocol for NLRR3 gene promoter and control regions, using appropriate primer sets (Supplementary Table S4).

Statistical analysis

Student *t* tests were employed to examine the possible association between *NLRR3* expression and other prognostic factors. The classification of high and low levels of *NLRR3*, *Miz-1*, and *MYCN* expression was determined on the basis of the mean value obtained from quantitative real-time PCR analysis. Kaplan–Meier survival curves were calculated, and survival distributions were compared by using the log-rank test. Cox regression models were used to search associations along with *NLRR3* expression, *MYCN*

expression, *Miz-1* expression, age, *MYCN* amplification status, INSS, *TrkA* expression, DNA index, origin, and survival. Statistical significance was considered if *P* value was less than 0.05. The statistical analysis was carried out by SPSS Statistical Software release 12.0.

Results

NLRR3 is upregulated during neuronal differentiation

It has been previously reported that the NBL cell lines exposed to ATRA undergo neuronal differentiation (32), accompanied by a marked decrease in the expression levels of *MYCN* (33). To examine the possible involvement of MYCN in the regulation of NLRR3 expression, the NBL-derived RTBM1 cells were treated with or without 5 μmol/L ATRA. As previously described (34), RTBM1 cells underwent neuronal differentiation with extensive neurite outgrowth in response to ATRA treatment (Fig. 1A). The induced differentiation was confirmed by the expression levels of *GAP43*, a marker of neuronal differentiation (35), which increased after ATRA treatment at both mRNA and protein levels (Fig. 1B and C). As expected, MYCN expression was significantly decreased after ATRA treatment and almost diminished at 6 days after treatment. Consistent with our previous observations (23), *NLRR3* was markedly upregulated at the mRNA and protein levels during the differentiation process. Similar results were also obtained from ATRA-treated SH-SY5Y cells (Supplementary Fig. S1A and B).

Inverse correlation between *MYCN* and *NLRR3* expressions

To further confirm a possible relationship between MYCN and NLRR3, we used MYCN-inducible SHEP21N cells originally derived from NBL (36) and treated with tetracycline to switch off the expression of MYCN. As shown in Fig. 2A, the reduced expression level of *MYCN* upon tetracycline treatment was confirmed by reverse transcriptase PCR (RT-PCR) and immunoblotting, whereas NLRR3 expression was increased after tetracycline treatment.

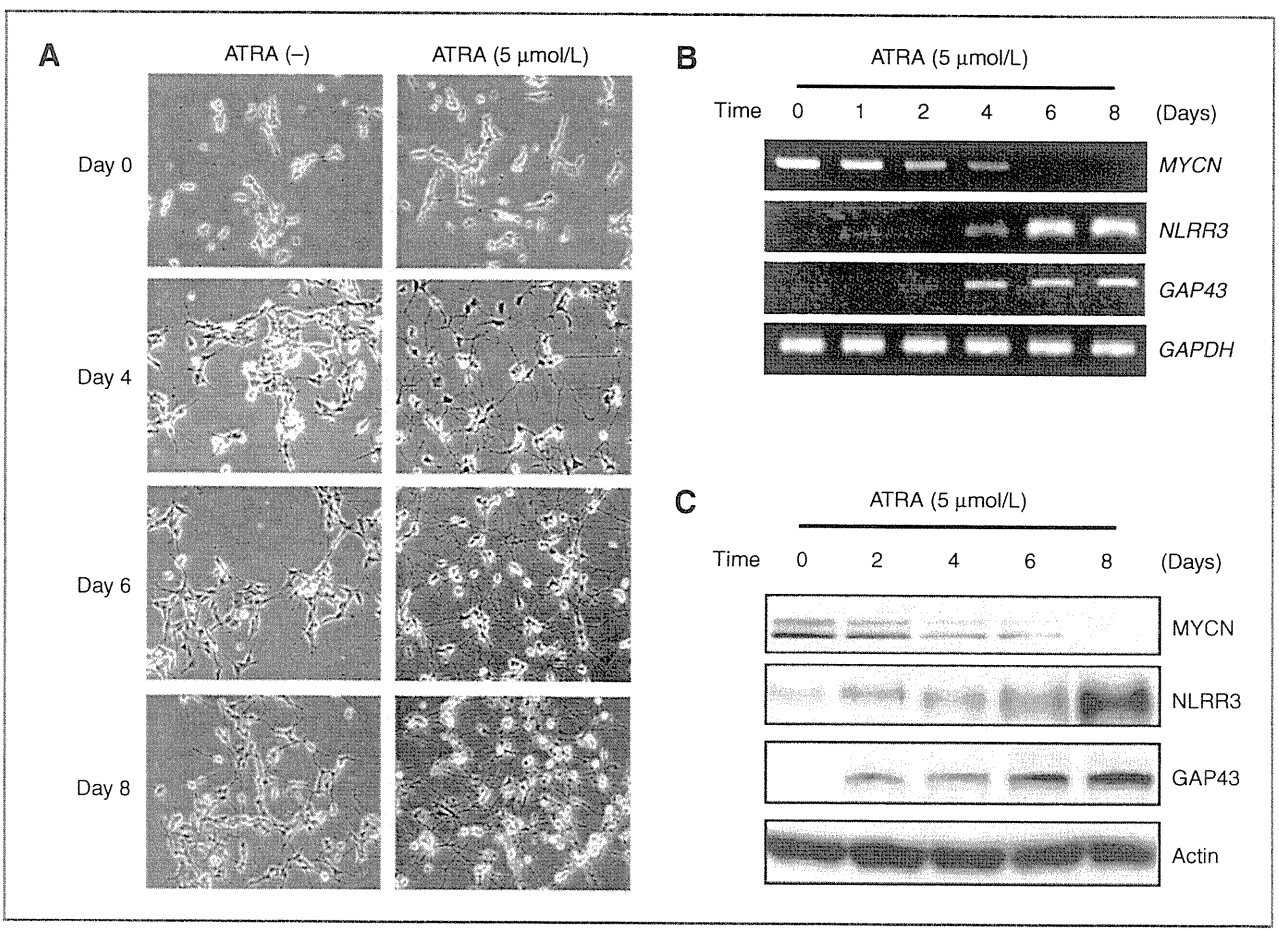

Figure 1. Opposite expression pattern of *NLRR3* and *MYCN* in differentiated RTBM1 cells in response to ATRA. A, ATRA-induced differentiation program in RTBM1 cells. Cells were treated with 5 μmol/L ATRA or left untreated. At the indicated time-periods after treatment with ATRA, neurite outgrowth was examined with a phase-contrast microscope. B and C, RT-PCR and immunoblot analysis for MYCN, NLRR3, and GAP43 in response to ATRA. RTBM1 cells were treated as in A. Total RNA and cell lysates were prepared and processed for RT-PCR (B) and immunoblotting with indicated antibodies (C). For RT-PCR, *GAPDH* was used as an internal control. For immunoblotting, actin was used as a loading control.

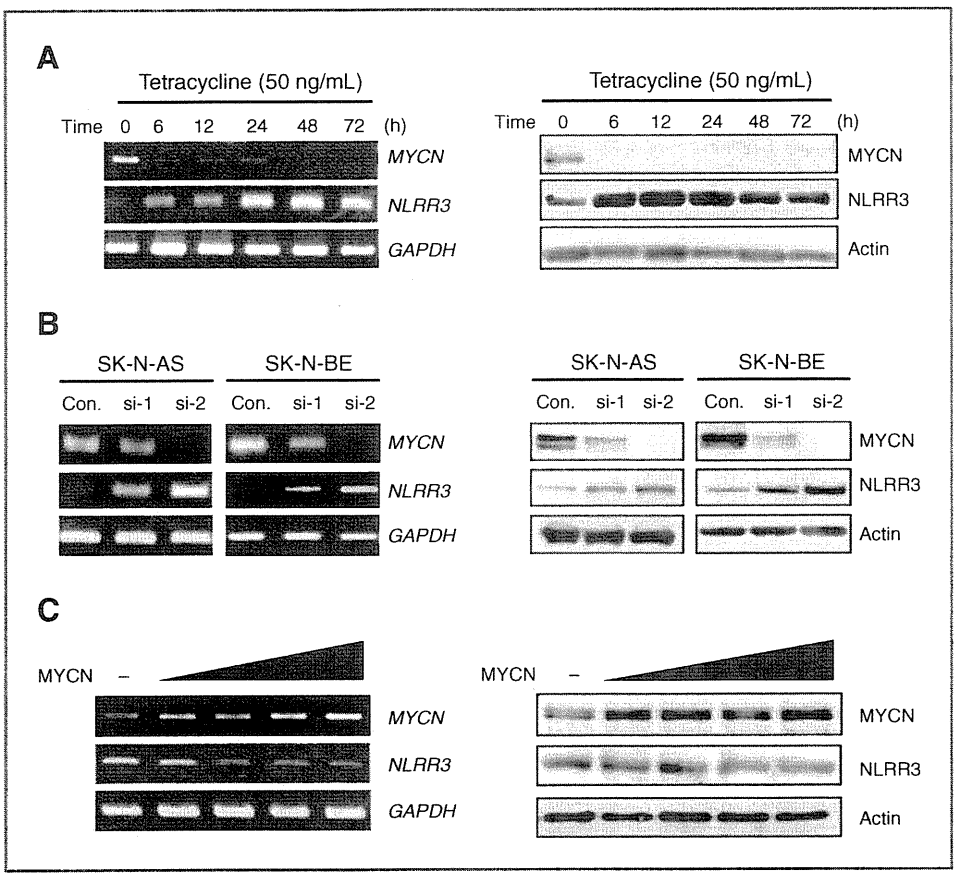

Figure 2. Inverse regulation of MYCN and NLRR3 in various NBL cell lines. A, RT-PCR and immunoblot analysis for MYCN and NLRR3 in SHEP21N cells maintained in the presence of tetracycline. At the indicated time points after the addition of tetracycline (50 ng/mL), total RNA and cell lysates were prepared and processed for RT-PCR (left) and immunoblotting with indicated antibodies (right). B, siRNA-mediated knockdown of the endogenous MYCN. SK-N-AS and SK-N-BE cells were transfected with control siRNA (Con.) or with 2 siRNA (si-1 and si-2) against MYCN. At 48 hours after transfection, total RNA and cell lysates were prepared and processed for RT-PCR (left) and immunoblotting with indicated antibodies (right). C, SH-SY5Y cells were transiently transfected with or without the increasing amounts of the expression plasmid encoding MYCN. Forty-eight hours after transfection, total RNA and cell lysates were prepared and processed for RT-PCR (left) and immunoblotting (right) with indicated antibodies. *GAPDH* was used as an internal control of RT-PCR and actin was used as a loading control for immunoblotting.

To examine whether MYCN and NLRR3 have an inverse functional relationship under these physiologic conditions, siRNA knockdown of the endogenous MYCN was carried out in 2 NBL cell lines, SK-N-AS cells with a single copy of *MYCN* and SK-N-BE cells with *MYCN* amplification. As shown in Fig. 2B, one of the siRNAs against *MYCN*, si-2, efficiently reduced endogenous expression of *MYCN* in both cell lines and resulted in an increased expression of NLRR3. SH-SY5Y cells with a single copy of *MYCN* also showed the similar result after siRNA-mediated knockdown of the endogenous MYCN (Supplementary Fig. S2A and B). These observations prompted us to examine whether MYCN can directly downregulate *NLRR3* expression. To address this issue, SH-SY5Y NBL cells were transfected with the expression plasmid encoding the *MYCN* gene. Forced expression of MYCN resulted in a dose-dependent decrease of NLRR3 expression both at the mRNA and protein levels (Fig. 2C), suggesting that *NLRR3* expression is negatively regulated by MYCN in NBL cells.

MYCN represses the promoter activity of *NLRR3* in association with Miz-1

According to the previous reports (19, 20, 37), Myc proteins repress its target genes by forming a complex with Miz-1. Under these conditions at low expression levels of Myc, Miz-1 activates transcription of the target genes by cooperating with other transcriptional cofactors and enhances cell differentiation (20). Therefore, we hypothesized that Miz-1 might be involved in the regulation of *NLRR3* expression. To prove this, we examined whether exogenously expressed Miz-1 upregulates *NLRR3* expression in SH-SY5Y cells. Figure 3A, left shows that *NLRR3* expression was upregulated by overexpression of Miz-1 in the same manner as a positive control, $p15^{Ink4b}$ expression, whereas expression of other NLRR family members, *NLRR1*

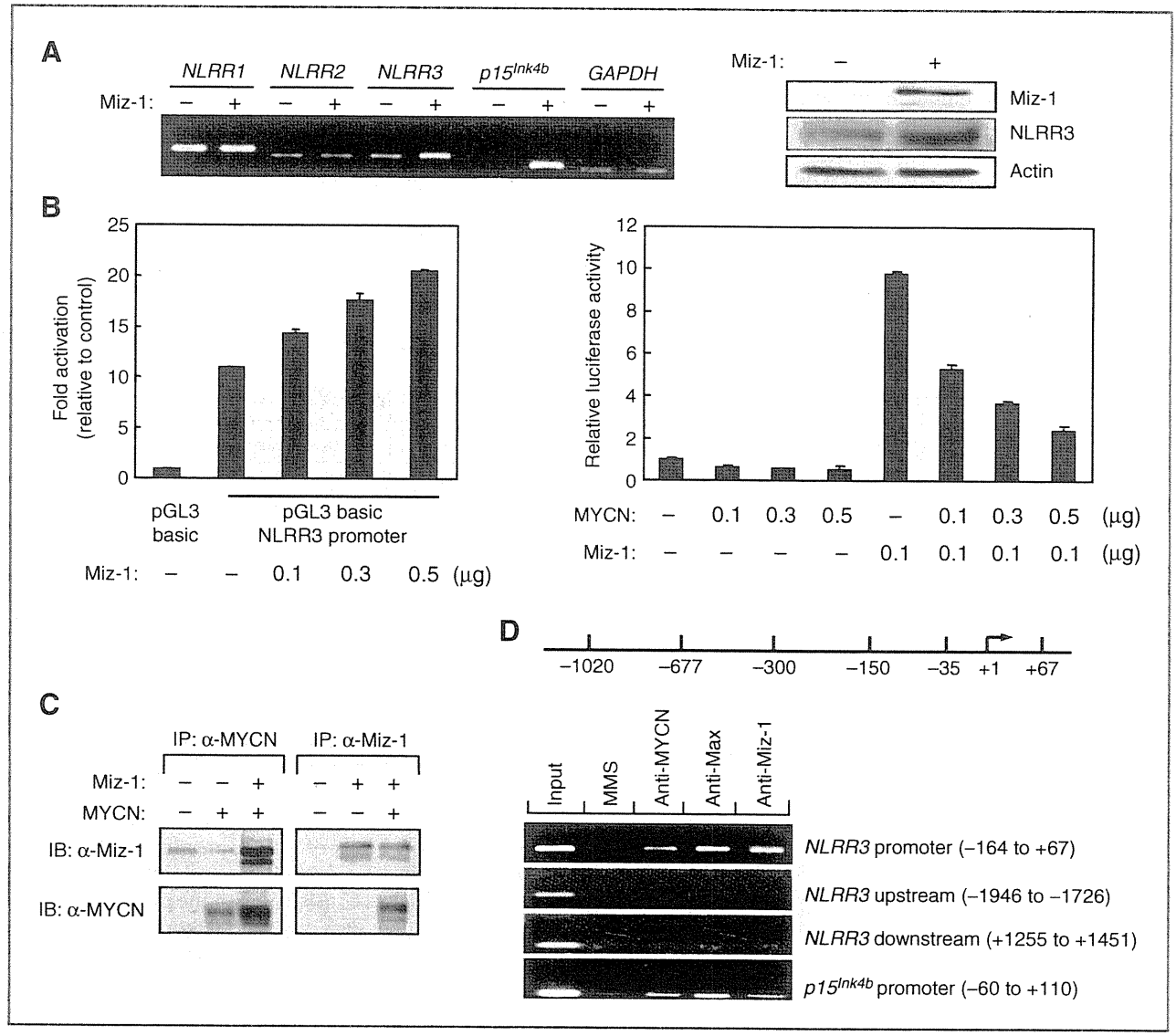

Figure 3. Regulation of the *NLRR3* promoter by MYCN and Miz-1. A, left, RT-PCR analysis showing expression of *NLRR1*, *NLRR2*, *NLRR3*, and $p15^{INk4b}$ in SH-SY5Y cells transiently transfected either with control or Miz-1–expressed plasmid. *GAPDH* was used as an internal control. Right, Western blot showing expression of *NLRR3* and *Miz-1* in SH-SY5Y cells transiently transfected either with control vector or with Miz-1 expressing vector. Actin was used as a loading control. B, left, Miz-1 enhances promoter activity of *NLRR3* in transient transfection assay. Data represent fold activation of the *NLRR3* promoter (−677 to +67) construct upon coexpression of increasing amounts of the expression plasmid for Miz-1 in SY5Y cells. Forty-eight hours after transfection, the cells were lysed and their relative luciferase activities were measured. Firefly luminescence signal was normalized on the basis of *Renilla* luminescence signal. Right, expression of MYCN reduces the basal activity of the *NLRR3* promoter and abrogates transactivation by Miz-1. SH-SY5Y cells were transiently cotransfected with or without constant amount of the expression plasmid for the Miz-1 and 0.1 μg of *NLRR3* promoter (−677 to +67) together with or without the increasing amounts of the expression plasmid for MYCN. The luciferase activity was determined as in B, left. Results are the mean of 3 independent experiments ± SD. C, interaction between MYCN and Miz-1 in NBL cells. Whole cell lysates prepared from SK-N-AS cells transfected with indicated vectors and immunoprecipitated (IP) with the monoclonal anti-MYCN antibody or with polyclonal anti–Miz-1 antibody. The immunoprecipates were analyzed by immunoblotting (IB) with the polyclonal anti–Miz-1 antibody or with monoclonal anti-MYCN antibody, respectively. D, ChIP analysis of SH-SY5Y cells was carried out by using the indicated antibody and PCR primers specific for the different part of *NLRR3* promoter (top 3 panels), upstream, downstream (middle 2 panels) regions of the *NLRR3* gene, and for $p15^{INk4b}$ promoter (bottom).

and *NLRR2*, showed no change. The increased expression of NLRR3 protein was also confirmed by Western blot analysis (Fig. 3A, right). This induction of NLRR3 by Miz-1 was also observed in SK-N-AS cells (Supplementary Fig. S3). To determine whether Miz-1 activates the *NLRR3* promoter, the region spanning exon 2 and 5′-upstream sequences of the *NLRR3* gene (nucleotide −1,020 to +67) was cloned and analyzed for promoter activity by using a luciferase reporter assay. The promoter deletion analysis showed that a nucleotide position between −677 and +67 gives maximum promoter activity (Supplementary Fig. S4A). The core promoter region (−35 to +67) also

showed higher promoter activity than other deletion mutants. In transient-cotransfection assays, simultaneous expression of Miz-1 increased the luciferase activities driven by the *NLRR3* promoter (−677 to +67; Fig. 3B, left).

On the contrary, overexpression of MYCN resulted in reduced activity of the *NLRR3* promoter (Supplementary Fig. S4B). These results suggest that Miz-1 and MYCN together contribute to the transcriptional regulation of the *NLRR3* gene. Indeed, the activation of the *NLRR3* promoter by exogenous Miz-1 expression in SH-SY5Y cells was suppressed by coexpression of MYCN in a dose-dependent manner (Fig. 3B, right). The luciferase activities driven by the core promoter region (−35 to +67) also showed a similar result (data not shown). It was reported that a transcriptional suppression of the MYCN-targeted genes occurs when MYCN forms a complex with Miz-1 and Max (19). To make certain of the physical interaction between MYCN and Miz-1, the whole cell lysates prepared from the SK-N-AS cells cotransfected with *MYCN* and *Miz-1* were subjected to an immunoprecipitation assay. As shown in Fig. 3C, coimmunoprecipitation using either MYCN or Miz-1 antibody confirmed that MYCN and Miz-1 formed a complex in SK-N-AS cells as previously reported in non-NBL cell lines (38). Moreover, ChIP analysis revealed that MYCN, Max, and Miz-1 were recruited onto the same promoter region of *NLRR3* (−164 to +67) in SH-SY5Y cells (Fig. 3D). Hence, MYCN negatively regulates *NLRR3* expression by forming a transcriptional complex with Miz-1 in NBL cells.

Increased expression of *NLRR3* and *Miz-1* in favorable neuroblastoma

In our previous report, *NLRR3* is highly expressed in favorable NBLs with a single copy of *MYCN* as compared with NBLs with *MYCN* amplification. To evaluate whether the expression pattern of *Miz-1*, *NLRR3*, and *MYCN* observed in NBL cell lines is consistent in primary NBLs, we analyzed expression levels of those 3 genes in 16 favorable (stages 1 or 2, high expression of *TrkA* and a single copy of *MYCN*) and 16 unfavorable (stages 3 or 4, low expression of TrkA and amplification of *MYCN*) NBL samples by semiquantitative RT-PCR. As shown in Supplementary Fig. S5A, *NLRR3* and *Miz-1* were expressed at higher levels in favorable NBLs than those in unfavorable tumors, whereas the levels of *MYCN* expression were predominantly high in the unfavorable tumors. The expression levels of *NLRR3* and *Miz-1* were also higher in the cell lines with a single copy of *MYCN* than those with *MYCN* amplification, indicating evidence of a positive correlation between *NLRR3* and *Miz-1* expressions and of an inverse correlation between *NLRR3* and *MYCN* expressions (Supplementary Fig. S5B). Those expression patterns were further assessed by immunohistochemistry for NLRR3, MYCN, and Miz-1 in primary NBL tissues (Supplementary Fig. S5C). We carried out immunohistochemical staining on all 11 available paraffin-embedded primary NBL tissues, including 5 NBLs with a single copy of *MYCN* and favorable histology according to INPC (39), 3 NBLs carrying a single copy of *MYCN* with unfavorable histology, and 3 NBLs with *MYCN* amplification and unfavorable histology. As shown in Supplementary Fig. S5C and Supplementary Table S1, the absence of MYCN amplification was associated with strong positive staining of NLRR3 and Miz-1 in all examined samples except one (case 8). All 3 NBLs with *MYCN* amplification showed weak staining for both NLRR3 and Miz-1.

Low expression of *NLRR3* and *Miz-1* is associated with an unfavorable outcome of neuroblastoma

To evaluate whether a statistically significant relationship exists between the patients' survival periods and the expression of *NLRR3*, *Miz-1*, or *MYCN* in primary NBLs, we quantitatively measured the expression levels of *NLRR3*, *Miz-1*, and *MYCN* mRNAs in 87 primary NBLs by using the quantitative real-time PCR method. The clinical features of each NBL samples are listed in Supplementary Table S2. As shown in Table 1, high levels of *NLRR3* expression were significantly associated with younger age ($P = 0.047$), single copy of *MYCN* ($P = 0.047$), favorable disease stages ($P = 0.041$), high levels of *TrkA* expression ($P = 0.042$), and diploid DNA index ($P = 0.003$), but not with tumor origin ($P = 0.933$). A high level of *Miz-1* expression was also significantly associated with younger age ($P = 0.004$), single copy of *MYCN* ($P = 0.004$), favorable disease stages ($P = 0.001$), and high levels of *TrkA* expression ($P = 0.001$), but not with DNA index ($P = 0.060$) and tumor origin ($P = 0.959$). In contrast, a high level of *MYCN* expression was significantly associated with *MYCN* amplification ($P = 0.0001$), advanced disease stages ($P = 0.0031$), low levels of *TrkA* expression ($P = 0.026$), and tumor origin ($P = 0.028$), but not with DNA index ($P = 0.079$), which is consistent with the previous reports (23, 40, 41). There was also a marginal association with patient age ($P = 0.063$). These results suggest that high expression of *NLRR3* and *Miz-1* is well associated with conventional prognostic markers predicting a favorable NBL outcome.

To examine whether the expression levels of *NLRR3*, *Miz-1* and/or *MYCN* have a prognostic significance in primary NBLs, we employed log-rank tests for gene-expression data (Supplementary Table S3). There were significant differences in survival rates in the groups of patients with high and low expression of *NLRR3*, *Miz-1*, and *MYCN*. Patients with high expression of *NLRR3* or *Miz-1* had a higher survival rate than patients with low expression of *NLRR3* or *Miz-1*, and such a difference in survival rate was statistically significant ($P = 0.0023$ and $P = 0.00060$, respectively). However, a patient with high *MYCN* expression was associated with a lower survival rate than that of the *MYCN* low subset ($P < 0.00001$; Supplementary Table S3). Figure 4 shows Kaplan–Meier cumulative survival curves for 87 patients with NBL in terms of expression of *NLRR3*, *Miz-1* and *MYCN*. High expression of *NLRR3* and that of *Miz-1* were significantly associated with good survival ($P = 0.0023$ and $P = 0.00060$, respectively; Fig. 4A, left and right). As already known, high expression of *MYCN*

Table 1. Correlation between expression of *NLRR3* or *MYCN* or *Miz-1* and other prognostic factors (Student *t* test)

		NLRR3		*MYCN*		*Miz-1*	
Variable	**No.**	**Mean ± SEM**	***P***	**Mean ± SEM**	***P***	**Mean ± SEM**	***P***
Age, y							
<1	32	0.043 ± 0.011	0.047[a]	0.034 ± 0.013	0.063	0.091 ± 0.019	0.004[a]
≥1	55	0.024 ± 0.003		0.141 ± 0.043		0.042 ± 0.007	
MYCN copy number							
Single copy	58	0.041 ± 0.006	0.047[a]	0.022 ± 0.016	0.0001[a]	0.077 ± 0.012	0.004[a]
Amplified	29	0.019 ± 0.004		0.222 ± 0.053		0.026 ± 0.004	
Tumor stage							
1, 2, 4s	34	0.043 ± 0.009	0.041[a]	0.007 ± 0.002	0.0031[a]	0.093 ± 0.017	0.001[a]
3, 4	53	0.024 ± 0.003		0.144 ± 0.036		0.039 ± 0.007	
TrkA expression							
High	24	0.047 ± 0.013	0.042[a]	0.009 ± 0.003	0.026[a]	0.104 ± 0.024	0.001[a]
Low	61	0.025 ± 0.004		0.125 ± 0.032		0.044 ± 0.006	
DNA index							
Diploidy	42	0.019 ± 0.003	0.003[a]	0.121 ± 0.037	0.079	0.049 ± 0.008	0.06
Aneuploidy	31	0.050 ± 0.010		0.034 ± 0.023		0.085 ± 0.019	
Tumor origin							
Adrenal gland	48	0.032 ± 0.007	0.933	0.135 ± 0.035	0.028[a]	0.059 ± 0.012	0.959
Others	39	0.032 ± 0.004		0.034 ± 0.025		0.060 ± 0.011	

[a]$P < 0.05$.

was strongly associated with a poor prognosis of NBL ($P < 0.00001$; Fig. 4A, middle). Remarkably, the combination of low levels of both *NLRR3* and *Miz-1* expressions showed a significantly worse prognosis as compared with the other combination, high *NLRR3* and *Miz-1* expressions ($P = 0.0012$; Fig. 4C). Furthermore, the combination of low expression of *NLRR3* and high expression of *MYCN* showed a significantly worse prognosis than the combination of high expression of *NLRR3* and low expression of *MYCN* ($P < 0.00001$; Fig. 4B). In NBLs with low expression of *MYCN*, the expression levels of *NLRR3* could segregate the prognosis into good and intermediate groups.

The univariate Cox regression analysis shown in Table 2 was employed to examine the individual relationship of each variable to survival. The results in Table 2 showed that *NLRR3* expression, *MYCN* expression, *Miz-1* expression, age, *MYCN* amplification, stage *TrkA* expression, and origin were of prognostic importance, supporting the results of the log-rank test. Moreover, the multivariate Cox models were fitted to assess the predictive importance of NLRR3 expression for survival after controlling other prognostic factors. The results in Table 2 showed that *NLRR3* expression was significantly associated with survival after controlling *TrkA* expression ($P = 0.0212$), suggesting that *NLRR3* expression was an independent prognostic factor from *TrkA* expression (Table 2). This suggests that *NLRR3* expression is associated with survival after controlling *MYCN* expression ($P = 0.0610$), *Miz-1* expression ($P = 0.1510$), *MYCN* amplification ($P = 0.1210$), and stage ($P = 0.1040$), and also supports that *NLRR3* expression could serve as a prognostic biomarker for NBL tumors dependent on both MYCN and Miz-1 expression as well as *MYCN* amplification.

Discussion

In primary human NBLs, *MYCN* is frequently amplified and thereby one of the most important prognostic factors. In this study, we found that *NLRR3* is a direct target of MYCN but its expression is negatively regulated by MYCN in association with Miz-1. In primary NBLs, both *NLRR3* and *Miz-1* are expressed at significantly high levels in favorable NBLs and downregulated in *MYCN*-amplified aggressive tumors.

In general, favorable NBL cells show more differentiated features than unfavorable cells (30). The treatment of NBL cells with ATRA induces neuronal differentiation accompanied with growth inhibition and reduction of *MYCN* expression (33). Under such conditions, *NLRR3* is induced while *MYCN* is decreased (Figs. 1 and 2). These results suggest a functional inverse relationship between MYCN and NLRR3 in cellular differentiation and tumor development. In some NBL cell lines, siRNA-mediated knockdown of endogenous MYCN caused NLRR3 induction; conversely, ectopic expression of MYCN resulted in a decreased expression of *NLRR3*. Hence, the inverse regulatory relationship between NLRR3 and MYCN may be present as a

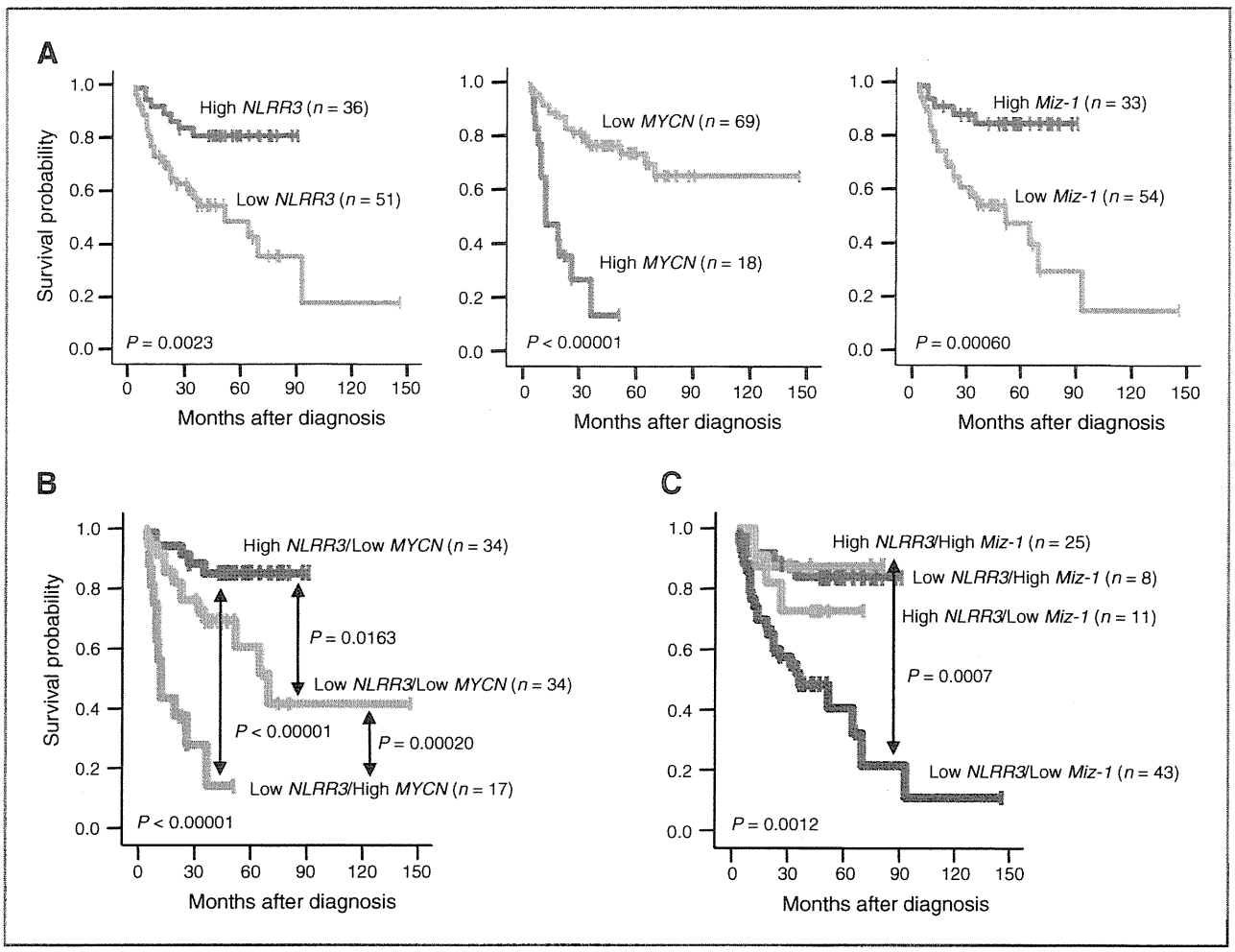

Figure 4. Real-time PCR analysis for the expression of *NLRR3*, *MYCN*, and *Miz-1* in 87 primary NBLs. Kaplan–Meier survival curves of patients with NBLs on the basis of higher or lower expression levels of *NLRR3* (A, left); *MYCN* (A, middle); *Miz-1* (A, right); *NLRR3* and *MYCN* (B); or *NLRR3* and *Miz-1* (C). In case of *NLRR3* and *MYCN* survival curve, high NLRR3/high MYCN group was excluded because this group consists of only 2 samples. Relative expression levels of *NLRR3* or *MYCN* or *Miz-1* mRNA were determined by calculating the ratio between *GAPDH* and *NLRR3* or *MYCN* or *Miz-1*.

consequence of MYCN-induced transcriptional downregulation of *NLRR3*.

MYCN protein is an important regulator of many cellular processes, including growth, proliferation, differentiation, and apoptosis (42). A part of these diverse cellular functions of MYCN may be due to the combined abilities of both activating and repressing transcription of the target genes (42). Transcriptional activation by MYCN occurs *via* dimerization with its partner protein, Max, and direct binding to specific DNA sequences named E-boxes. MYCN directly binds and stimulates the expression of approximately 4,000 of the E-box containing genes (43). Although heterodimerization of Max with MYCN is necessary to regulate gene expression, the other proteins including *Miz-1* may bind to C-terminal MYCN in addition to Max (19, 20, 44). Concurrent binding of these factors redirects the MYCN/Max dimer to noncanonical sites such as the initiator element, where this complex might prevent the efficient binding of basal transcriptional machinery or coactivators necessary for transactivation, resulting in repression of gene expression (38, 44). The dimerization with MYCN switches Miz-1 from a transcriptional activator to a repressor of the target genes, likely by preventing the interaction of Miz-1 with its own coactivator (19, 20). Several studies have shown that Miz-1 binds and activates the promoter of several genes, including $p15^{INK4b}$ and $p21^{CIP1}$, and the transactivation can be negatively regulated by its association with MYCN (16, 17, 29). Regarding the reduction of NLRR3 expression observed in this study, Miz-1 seems to be a key molecule forming a transcription factor complex with MYCN. Because Miz-1 itself acts as an activator of *NLRR3* promoter, *NLRR3* expression may be switched on and off through Miz-1 in the absence and presence of MYCN, respectively. Although the expression levels of Miz-1 in unfavorable NBLs are relatively low, its amount still may be enough to act with MYCN to inhibit transactivation of *NLRR3* in NBLs.

Table 2. Multiple Cox regression model using NLRR3 expression and dichotomous factors of MYCN expression, Miz-1 expression, age, MYCN amplification, stage, TrkA expression, and origin ($n = 87$)

Model	Factor	*P*	HR (95% CI)
Univariate analysis			
A	*NLRR3* mRNA expression (high vs. low)	0.0041[a]	0.291 (0.125–0.678)
B	*MYCN mRNA* expression (high vs. low)	<0.0001[a]	5.050 (2.450–10.40)
C	*Miz-1* mRNA expression (high vs. low)	0.0021[a]	0.212 (0.080–0.561)
D	Age (≥1 vs. <1 y)	0.0161[a]	0.309 (0.119–0.803)
E	*MYCN* amplification (single copy vs. amplified)	<0.0001[a]	4.628 (2.281–9.387)
F	Stage (1,2,4s vs. 3,4)	0.0010[a]	12.66 (3.023–53.09)
G	*TrkA* expression (high vs. low)	0.0070[a]	7.180 (1.714–30.07)
H	Origin (adrenal gland vs. others)	0.0480[a]	2.125 (1.005–4.491)
Multivariate analysis			
A	*NLRR3* mRNA expression (high vs. low)	0.061	0.424 (0.172–1.041)
	MYCN mRNA expression (high vs. low)	0.0011[a]	3.707 (1.735–7.921)
B	*NLRR3* mRNA expression (high vs. low)	0.151	0.503 (0.198–1.283)
	Miz-1 mRNA expression (high vs. low)	0.0301[a]	0.304 (0.104–0.893)
C	*NLRR3* mRNA expression (high vs. low)	0.0150[a]	0.347 (0.148–0.814)
	Age (≥1 vs. <1 y)	0.053	0.384 (0.146–1.013)
D	*NLRR3* mRNA expression (high vs. low)	0.121	0.545 (0.253–1.173)
	MYCN amplification (single copy vs. amplified)	0.0001[a]	3.940 (1.893–8.203)
E	*NLRR3* mRNA expression (high vs. low)	0.104	0.493 (0.210–1.156)
	Stage (1, 2, 4s vs. 3, 4)	0.0020[a]	10.108 (2.359–43.309)
F	*NLRR3* mRNA expression (high vs. low)	0.0212[a]	0.361 (0.152–0.863)
	TrkA expression (high vs. low)	0.0163[a]	5.892 (1.395–24.901)
G	*NLRR3* mRNA expression (high vs. low)	0.0070[a]	0.308 (0.132–0.720)
	Origin (adrenal gland vs. others)	0.084	1.937 (0.914–4.104)

NOTE: All variables with 2 categories. HR shows the relative risk of death of first category relative to the second.
[a]$P < 0.05$.

Inhibition of cellular differentiation is one of the well-known biological functions of MYCN. Because differentiated NBL cells have a high expression of NLRR3 instead of MYCN, the reduced expression of NLRR3 in undifferentiated, unfavorable NBL cells may propose an important component of the mechanism by which MYCN functions against cell differentiation. As ectopic expression of NLRR3 induced morphologic changes indicative of neuronal differentiation accompanying with neurite outgrowth (data not shown), the downregulation of NLRR3 by MYCN might contribute to the well-documented stimulation of cell proliferation by MYCN. Although there are MYCN target genes that are potentially involved in cell-cycle progression, including *α-prothymosin, ornithine decarboxylase, MCM7, ID2, MDM2,* and *NLRR1* (27, 36, 45–47), suppression of NLRR3 might have an additive effect on NBL cell proliferation. Our log-rank test showed that expression of NLRR3 is well associated with a favorable prognosis, suggesting its involvement in NBL differentiation. Of more interest, NLRR3 and NLRR1 seem to function oppositely in NBL. Thus, the expression of NLRR3 is a new prognostic indicator of NBL and may be involved in regulating the biology of the tumor.

Collectively, our present findings suggest that the repression of NLRR3 mediated by MYCN requires an association with Miz-1 and also contributes to the favorable outcome of NBLs. The expression pattern of NLRR3, Miz-1, and MYCN might play an important role in defining the clinical behavior of NBLs. Because NLRR3 is an orphan receptor, the future discovery of its ligand(s) may unveil the molecular mechanism of tumorigenesis, differentiation, and proliferation of NBL. Further investigation is necessary to clarify whether NLRR3 is an important primary cue for developing novel diagnostic and therapeutic strategies against high-risk NBLs.

Disclosure of Potential Conflicts of interest

No potential conflicts of interest were disclosed.

Acknowledgments

The authors thank Drs. Y. Nakamura and E. Isogai (Chiba Cancer Center Research Institute, Chiba, Japan) for their outstanding technical assistance, and Dr. Hiroki Nagase (Chiba Cancer Center Research Institute, Chiba, Japan) and Ms. Paula D. Jones (Roswell Park Cancer Institute, Buffalo, NY) for critical reading of the article.

Grant Support

This work was supported in part by a grant-in-aid from the Ministry of Health, Labour and Welfare for Third Term Comprehensive Control Research for Cancer (A. Nakagawara), a grant-in-aid for Scientific Research on Priority Areas from the Ministry of Education, Culture, Sports, Science and Technology, Japan (A. Nakagawara), and a grant-in-aid for Scientific Research from the Japanese Society for the Promotion of Science (A. Takatori and A. Nakagawara).

The costs of publication of this article were defrayed in part by the payment of page charges. This article must therefore be hereby marked *advertisement* in accordance with 18 U.S.C. Section 1734 solely to indicate this fact.

Received February 3, 2011; revised August 3, 2011; accepted August 9, 2011; published OnlineFirst September 9, 2011.

References

1. Westemann F, Schwab M. Genetic parameters of neuroblastomas. Cancer Lett 2002;184:127–47.
2. Brodeur GM, Nakagawara A. Molecular basis of clinical heterogeneity in neuroblastoma. Am J Pediatr Hematol Oncol 1992;14: 111–6.
3. Nakagawara A, Arima M, Azar CG, Scavarda NJ, Brodeur GM. Inverse relationship between trk expression and N-myc amplification in human neuroblastomas. Cancer Res 1992;52:1364–68.
4. Nakagawara A, Arima-Nakagwara M, Scavarda NJ, Azar CG, Cantor AB, Brodeur GM. Association between high levels of expression of the TRK gene and favorable outcome in human neuroblastoma. New Engl J Med 1993;328:847–54.
5. Nakagawara A, Azar CG, Scavarda NJ, Brodeur GM. Expression and function of TRK-B and BDNF in human neuroblastomas. Mol Cell Biol 1994;14:759–67.
6. Nakagawara A, Arima-Nakagawara M, Azar CG, Scavarda NJ, Brodeur GM. Clinical significance of expression of neurotrophic factors and their receptors in neuroblastoma. Prog Clin Biol Res 1994;385: 155–61.
7. Seeger RC, Brodeur GM, Sather H, Dalton A, Siegel SE, Wong KY, et al. Associations of multiple copies of the N-myc oncogene with rapid progression of neuroblastomas. New Engl J Med 1985;313: 1111–6.
8. Kohl NE, Gee CE, Alt FW. Activated expression of the N-myc gene in human neuroblastomas and related tumors. Science 1984;226: 1335–7.
9. Nisen PD, Waber PG, Rich MA, Pierce S, Garvin JR, Gilbert F, et al. N-myc oncogene RNA expression in neuroblastoma. J Natl Cancer Inst 1988;80:1633–7.
10. Slavc I, Ellenbogen R, Jung WH, Vawter GF, Kretschmar C, Grier H, et al. Myc gene amplification and expression in primary human neuroblastoma. Cancer Res 1990;50:1459–63.
11. Seeger RC, Wada R, Brodeur GM, Moss TJ, Bjork RL, Sousa L, et al. Expression of N-myc by neuroblastomas with one or multiple copies of the oncogene. Prog Clin Biol Res 1988;271:41–9.
12. Schwab M, Ellison J, Busch M, Rosenau W, Varmus HE, Bishop JM. Enhanced expression of the human gene N-myc consequent to amplification of DNA may contribute to malignant progression of neuroblastoma. Proc Natl Acad Sci U S A 1984;81:4940–4.
13. Cohn SL, Tweddle DA. MYCN amplification remains prognostically strong 20 years after its "clinical debut". Eur J Cancer 2004;40: 2639–42.
14. Strieder V, Lutz W. Regulation of N-myc expression in development and diseases. Cancer Lett 2002;180:107–19.
15. Kouzarides T, Ziff E. The role of the leucine zipper in the fos-jun interaction. Nature 1988;336:646–51.
16. Landschulz WH, Johnson PF, Mcknight SL. The leucine zipper: a hypothetical structure common to a new class of DNA binding proteins. Science 1988;240:1759–64.
17. Alex R, Sozeri O, Meyer S, Dildrop R. Determination of the DNA sequence recognized by the bHLH-zip domain of the N-Myc protein. Nucleic Acids Res 1992;20:2257–63.
18. Blackwood EM, Kretzner L, Eisenman RN. Myc and Max function as a nucleoprotein complex. Curr Opin Genet Dev 1992;2:227–35.
19. Staller P, Peukert K, Kiermaier A, Seoane J, Lukas J, Karsunky H, et al. Repression of p15INK4b expression by Myc through association with Miz-1. Nature Cell Biol 2001;3:392–9.
20. Wu S, Cetinkaya C, Munoz-Alonso MJ, Von der Lehr N, Bahram F, Beuger V, et al. Myc represses differentiation-induced p21CIP1 expression via Miz-1-dependent interaction with the p21 core promoter. Oncogene 2003;22:351–60.
21. Zhang J, Li F, Liu X, Shen L, Liu J, Su J, et al. The repression of human differentiated-related gene NDRG2 expression by Myc via Miz-1 dependent interaction with the NDRG2 core promoter. J Biol Chem 2006;281:39159–68.
22. Koppen A, Ait-Aissa R, Hopman S, Koster J, Haneveld F, Versteeg R, et al. Dickkopf-1 is down-regulated by MYCN and inhibits neuroblastoma cell proliferation. Cancer Lett 2007;256:218–28.
23. Hamano S, Ohira M, Isogai E, Nakada K, Nakagawara A. Identification of novel human neuronal leucine-rich repeat (hNLRR) family genes and inverse association of expression of Nbla10449/hNLRR-1 and Nbla10677/hNLRR-3 with the prognosis of primary neuroblastomas. Int J Oncol 2004;24:1457–66.
24. Ohira M, Morohashi A, Inuzuka H, Shishikura T, Kawamoto T, Kageyama H, et al. Expression profiling and characterization of 4200 genes cloned from primary neuroblastomas: identification of 305 genes differentially expressed between favorable and unfavorable subsets. Oncogene 2003;22:5525–36.
25. Hayata T, Uochi T, Asashima M. Molecular cloning of XNLRR-1, a Xenopus homolog of mouse neuronal leucine-rich repeat protein expressed in the developing Xenopus nervous system. Gene 1998;221:159–66.
26. Fukamachi K, Matsuoka Y, Ohno H, Hamaguchi T, Tsuda H. Neuronal leucine-rich repeat protein-3 amplifies MAPK activation by epidermal growth factor through a carboxyl-terminal region containing endocytosis motifs. J Biol Chem 2002;277:43549–52.
27. Hossain MS, Ozaki T, Wang H, Nakagawa A, Takenobu H, Ohira M, et al. N-MYC promotes cell proliferation through a direct transactivation of neuronal leucine-rich repeat protein-1 (NLRR1) gene in neuroblastoma. Oncogene 2008;27:6075–82.
28. Ishii N, Wanaka A, Tohyama M. Increased expression of NLRR-3 mRNA after cortical brain injury in mouse. Molecular Brain Research 1996;40:148–52.
29. Brodeur GM, Pritchard J, Berthold F, Carlsen NL, Castel V, Castelberry RP, et al. Revisions of the international criteria for neuroblastoma. Diagnosis, staging, and response to treatment. J Clin Oncol 1993;11:1466–77.
30. Matsumura T, Iehara T, Sawada T, Tsuchida Y. Prospective study for establishing the optimal therapy of infantile neuroblastoma in Japan. Med Pediatr Oncol 1998;31:210.
31. Kaneko M, Nishihira H, Mugishima H, Ohnuma N, Nakada K, Kawa K, et al. Stratification of treatment of stage 4 neuroblastoma patients based on N-myc amplification status. Study Group of Japan for Treatment of Advanced Neuroblastoma, Tokyo, Japan. Med Pediatr Oncol 1998;31:1–7.
32. Melino G, Thiele CJ, Knight RA, Piacentini M. Retinoids and the control of growth/death decisions in human neuroblastoma cell lines. J Neurooncol 1997;31:65–83.
33. Thiele CJ, Reynolds CP, Israel MA. Decreased expression of N-myc precedes retinoic acid-induced morphological differentiation of human neuroblastoma. Nature 1985;313:404–6.
34. Niizuma H, Nakamura Y, Ozaki T, Nakanishi H, Ohira M, Isogai E, et al. Bcl-2 is a key regulator for the retinoic acid-induced apoptopic cell death in neuroblastoma. Oncogene 2006;25:5046–55.
35. Bjelfman C, Meyerson G, Cartwright CA, Mellstrom K, Hammerling U, Pahlman S. Early activation of endogenous pp60src kinase activity during neuronal differentiation of cultured human neuroblastoma cells. Mol Cell Biol 1990;10:361–70.

36. Lutz W, Stohr M, Schurmann J, Wenzel A, Lohr A,Schwab M. Conditional expression of N-myc in human neuroblastoma cells increases expression of α-prothymosin and ornithine decarboxylase and accelerates progression into S-phase after mitogenic stimulation of quiescent cells. Oncogene 1996;13:803–12.
37. Chen L, Peng Z, Bateman E. In vivo interactions of the Acanthamoeba TBP gene promoter. Nucleic acids Res 2004;32: 1251–60.
38. Peukert K, Staller P, Schneider A, Carmichael G, Hanel F,Eilers M. An alternative pathway for gene regulation by Myc. EMBO J 1997;16: 5672–86.
39. Shimada H, Ambros IM, Dehner LP, Hata J, Joshi VV, Roald B, et al. The International Neuroblastoma Pathology Classification (the Shimada System). Cancer 1999;86: 364–72.
40. Ikegaki N, Gotoh T, Kung B, Riceberg JS, Kim DY, Zhao H, et al. De novo identification of MIZ-1 (ZBTB17) encoding a MYC-interacting zinc-finger protein as a new favorable neuroblastoma gene. Clin Cancer Res 2007;13:6001–9.
41. Tang XX, Zhou H, Kung B, Kim DY, Hicks SL, Cohn SL, et al. The MYCN enigma: significance of MYCN expression in neuroblastoma. Cancer Res 2006;66:2826–33.
42. Pelengaris S, Khan M, Evan G. c-MYC: more than just a matter of life and death. Nat Rev Cancer 2002;2:764–76.
43. Levens DL. Reconstructing MYC. Genes dev 2003;17:1071–7.
44. Wanzel M, Herold S, Eilers M. Transcriptional repression by Myc. Trends Cell Biol 2003;13:146–50.
45. Shohet JM, Hicks MJ, Plon SE, Burlingame SM, Stuart S, Chen SY, et al. Minichromosome maintenance protein MCM7 is a direct target of the MYCN transcription factor in neuroblastoma. Cancer Res 2002;62:1123–8.
46. Iasorella A, Noseda M, Beyna M, Yokota Y, Iavarone A. Id2 is a retinoblastoma protein target and mediates signaling by Myc oncoproteins. Nature 2000;407:592–8.
47. Slack A, Chen Z, Tonelli R, Pule M, Hunt L, Pession A, et al. The p53 regulatory gene MDM2 is a direct transcriptional target of MYCN in neuroblastoma. Proc Natl Acad Sci U S A 2005;102:731–6.

より良い診療を目指して 他診療科との連携

17. 小児の固形腫瘍

七野浩之* 谷ケ崎博* 陳基明* 麦島秀雄*

はじめに

おそらく医療関係者でさえも小児がんは「不治の病」であるという印象を持たれるのではないだろうか。実際に世界で最も優れた治療成績を報告している米国でも1960年代には28%の生存率に過ぎなかった。しかしその後の目覚ましい治療法の進歩により1990年代には75%を達成し，さらに改善を続けている[1]。現在では治癒後の後遺症が少なく質の高い生存が得られるような治療法の開発が研究者・臨床家の間の目標となっている。

眼科領域には小児がんの原発や転移がみられるだけではなく，種々の関連した合併症が出現する。眼科との密接な連携がなければ小児がんの治療は成り立たず，質の高い生存も獲得されない。小児がんにとっては眼科領域は非常に重要である。

I. 小児固形腫瘍の背景

❶ 頻　度

小児がんとは，小児の血液性悪性腫瘍と固形腫瘍の総称である。日本の小児がんの頻度は，1年間に，血液性悪性腫瘍1,000人と固形腫瘍600人の合計約1,600人の登録と報告されている（2010年日本小児血液学会・日本小児がん学会合同開催学術集会における両学会の登録事業報告）。これに固形腫瘍のうちで最も多い脳腫瘍の登録数が加わるものと考えられ，合計ではおおよそ2,000人の発生と推測される。これは小児人口8,500人にひとりの割合である。成人がんが年に60万人，人口200人にひとりの発生であるのと比較すると非常に少ない。しかし小児がんは，その発生や病因・病態の研究あるいは多剤併用化学療法や集学的治療などの臨床研究において，成人がんにも多大な影響を与え，がん治療の進歩に大きく寄与しているといってよいであろう。

❷ 種　類

小児の固形腫瘍は小児がん全体の60%を占め，残りの40%は白血病と悪性リンパ腫である[1]。固形腫瘍のほとんどは肉腫（sarcoma）であり，成人で一般的な上皮性腫瘍は1～2%に過ぎない。肉腫は胎生期に種々の細胞が遊走移動し臓器を形成する過程で何らかの要因により腫瘍化したものと推測され，全身の臓器・部位に発生する。頭蓋内の脳腫瘍（頻度は小児がん全体の約20%），眼の網膜芽細胞腫（約3%），

* Hiroyuki SHICHINO, Hiroshi YAGASAKI, Motoaki CHIN, Hideo MUGISHIMA　日本大学医学部小児科学系小児科学分野

肝の肝芽腫（約3%），腎の腎芽腫（約3%），骨の骨肉腫（約4%）といった特定の臓器に発生するものだけでなく，全身の軟部組織や結合織にも種々の固形腫瘍が発生する。交感神経幹に添い発生する神経芽腫（約9%）は，頸部・後縦隔・副腎・後腹膜・骨盤腔に原発するだけでなく，肝・リンパ節・皮膚・頭蓋内・腎・肺・骨・骨髄・眼窩など全身に転移部位を認める。横紋筋肉腫やユーイング（Ewing）肉腫（合わせて約6%）・ランゲルハンス（Langerhans）細胞組織球症・悪性リンパ腫（約11%）・胚細胞性腫瘍（約8%）などは全身のどの臓器・部位にも原発し，眼科領域に発生することも少なくない。病態は非常に多様性に富んでいる。

❸予　後

小児がん全体の予後は，現在の日米欧では概ね75%以上の生存率を達成するようになった[1]。それは当初から世界的協力体制による多施設共同臨床研究を行い，多剤併用化学療法に放射線療法および外科療法を組み合わせた集学的治療に取り組んできた成果と考えられる。さらに，小児がんが化学療法や放射線療法に高い感受性を有していることも寄与している。

小児がんは全体として75%以上の治癒率を達成してはいるが，その種類・病期・リスクにより治療成績は大きく異なる。低リスク群と考えられる標準危険群急性リンパ性白血病や腎芽腫・網膜芽細胞腫・Hodgkin病などは，80～90%以上の無病生存率が達成されている。一方，高リスク群と考えられる高危険群急性リンパ性白血病や遠隔転移を認める種々の固形腫瘍の予後は20～40%にとどまる。今後も引き続き基礎および臨床研究が必要とされている。

❹長期生存者

小児がん患者は，幼小児期に治療が行われ，その後70～80年の長期間の生命予後が期待されるようになった。彼らが小児がん治療を受けた時期は，出生直後から10代前半という成長発達期にあたるため，その影響は深刻で長期に及んでいる[2]。

最も重要なことは，小児がんに対する治療が終了しても，彼らの生命予後は小児がん非経験者に比べて不良であることである。小児がん非経験者群（小児がん経験者の兄弟）の生存率が95%以上なのに対し，小児がん経験者群では80%と低いことが報告されている。その主因は小児がんの再発であるが，それも治療終了後15年までで減少する。それ以後は小児がん治療の影響による長期的な後遺症・合併症が主因となる。すなわち循環器合併症や呼吸器合併症，あるいは二次がんなどである。二次がんには甲状腺がん・皮膚がん・乳がん・脳腫瘍などが多く，その発生率は治療30年後には15%にも達している[2]。

また，低身長・思春期早発症・甲状腺機能低下症・性腺機能障害などの内分泌障害や，肥満や高脂血症などのメタボリック症候群，心筋症やうっ血性心不全・不整脈などの循環器疾患，白内障や視力障害などの眼科領域の障害，聴力障害や副鼻腔炎などの耳鼻科領域の障害，歯牙の形成不全や歯列不整などの歯科的問題，呼吸器系の障害，腎機能障害，婦人科領域の障害，頭髪や皮膚炎などの皮膚科領域の障害，神経学的障害，心理学的障害，認知学的障害などのさまざまな治療関連有害事象が起こり，これに成人期特有の疾患も加わり，さらに問題が複雑になっている。

成人となった小児がん経験者は，日本でも約10万人，成人人口1,000人にひとりの割合と推定される。多数の長期生存者の複雑な問題を小児血液腫瘍専門医だけでフォローすることは難しく，成人を診療する諸領域の医療関係者の協力が必要である。

II. 代表的な小児の固形腫瘍と眼科領域について

❶ 網膜芽細胞腫

網膜芽細胞腫は小児がんの3%程度を占める。13番染色体長腕バンド14(13q14)に存在する*RB1*遺伝子の変異により発生する[3]。*RB1*遺伝子は癌抑制遺伝子で，この変異による機能喪失が発症の契機となる。全体の40%は遺伝性で生殖細胞系変異を持ち，このうち家族歴があるのは15%，散発例は85%である。非遺伝性では体細胞変異を持つ。遺伝性では多くが1歳未満で発症し，両側性であり，眼球内に複数の腫瘍を持つ。非遺伝性では2〜3歳に多く，ほとんどが片側性で，眼球内の腫瘍は単数である。症状は白色瞳孔，斜視，結膜充血，視力低下，眼瞼腫脹，眼瞼突出などである。硝子体出血を起こすと瞳孔が黒色に見えることもある。

診断は眼底検査にX線CT(computed tomography)検査およびMRI(magnetic resonance imaging)検査を行い，眼内腫瘍の大きさ，位置，数，眼球外浸潤の有無を検索し病期を決定する。Neuron specific enolase(NSE)が上昇することがあるが腫瘍マーカーとしては不適当である。眼球外浸潤が疑われる場合には骨髄検査および髄液検査を行う。

眼球外腫瘍例では救命を優先し，治療は腫瘍を可能な限り切除し，眼窩内容除去を行い，術後に放射線照射あるいは化学療法を行う。眼球内腫瘍例では，眼球摘出を行う場合と，眼球を温存する場合がある。眼球摘出の適応は，腫瘍が進行し治療後の視力が回復できない場合，視神経浸潤・強膜浸潤など眼球外進展が強く疑われる場合，緑内障・内眼炎を併発し全身状態が不良の場合，家族が眼球温存を希望しない場合である。術後の病理学的検索により化学療法が決定される。上記の眼球摘出の適応がなく家族が眼球温存を希望する場合には，温存治療の可能性が検討される。温存治療としては，放射線外照射，全身化学療法，局所療法としてのレーザー治療・冷凍凝固・小線源治療，局所化学療法などがある。アメリカでの眼球摘出率は片側腫瘍の場合75%である。

日本での予後は5年生存率93%，10年生存率90%と良好である。遺伝性例では全身の*RB1*遺伝子の変異があるため，二次がんの発症率が高いと報告されている。また両眼性網膜芽細胞腫の場合には松果体腫瘍の合併が認められることがあり，三側性網膜芽細胞腫と呼ばれる。

❷ 横紋筋肉腫

横紋筋肉腫は未分化間葉系組織より発生し，横紋筋の表現型を有する軟部組織腫瘍である[4]。全身に発生し，小児がんの3%程度を占め，日本では年間発生数は60〜80例と推定される。約2/3は6歳以下の発症である。臨床症状は腫瘤関連の症状で，発生部位により異なる。

病理組織学的に胎児型(60%)・胞巣型(20%)・多形型・退形成型・硬化型に分類され，胎児型は予後良好，胞巣型は予後不良である。また分子生物学的因子として，胞巣型では*PAX3-FOXO1a*や*PAX7-FOXO1a*キメラ遺伝子を発現することが多く予後不良である。NSEが上昇するが腫瘍マーカーとしては不適当である。

術前病期分類，初回手術での残存腫瘍の程度(グループ分類)，腫瘍発生部位(予後良好部位には眼窩・眼瞼・傍髄膜を除く頭頸部・膀胱と前立腺を除く泌尿生殖器・胆道が含まれ，予後不良部位には傍髄膜・膀胱・前立腺・四肢・体幹が含まれる)と診断時年齢(10歳未満か以上か)を組み合わせてリスク分類を行い，低・中間・高リスクに分類し治療方針を決定する。

治療の基本は，全摘が可能であれば外科切除が第一で，その後に化学療法と放射線療法を組み合わせた集学的治療を行う。全摘が不能の場合には生検にとどめ，化学療法後に外科切除が

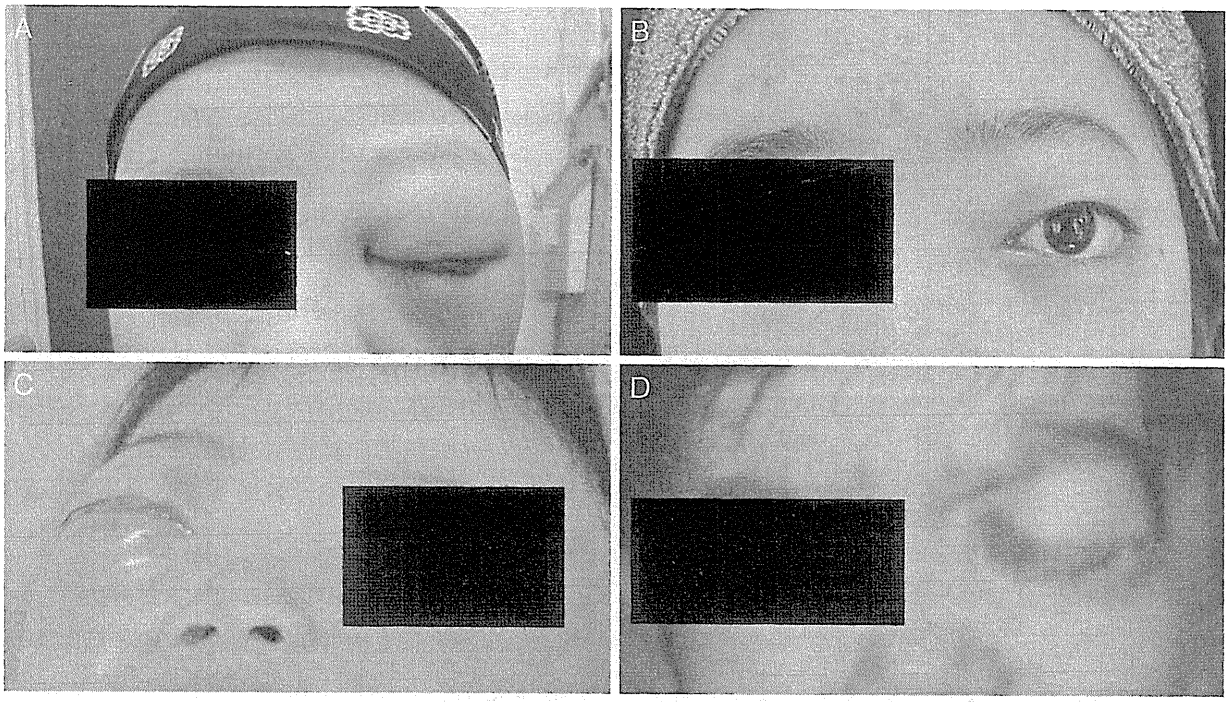

図1　眼球突出

A：ユーイング肉腫の左側頭骨骨転移例
左眼球突出に加え左眼周囲の腫脹と左上眼瞼の発赤を併せて認める。
B：横紋筋肉腫の左上顎洞・篩骨洞原発例
眼窩の骨を破壊し眼窩内に侵入しているため，左眼球突出を認める。
C：横紋筋肉腫の右眼窩内原発例
右眼球突出に加え右上下眼瞼腫脹と発赤を認める。
D：横紋筋肉腫の左眼窩内原発例
左眼球突出に加え左上眼瞼腫脹と出血斑を認める。

行われる。化学療法はvincristine（VCR）+ actinomycin D + cyclophosphamide（CPA）によるVAC療法が標準的治療である。

アメリカ横紋筋肉腫研究グループ（IRSG）では1972年から臨床研究を行い，全体の5年無病生存率はIRS-Iで55％，Ⅱで63％，Ⅲで71％，Ⅴで78％以上としだいに改善されてきている。日本横紋筋肉腫研究グループ（JRSG）は2004年から多施設共同研究を行っている。現在の期待生存率は，低リスク群は90％以上，中間リスク群は70％，高リスク群では20～30％と推測している。

横紋筋肉腫は眼科領域にも原発し，眼窩や眼瞼にみられる（**図1，2**）。症状は眼球突出・眼瞼周囲浮腫，眼瞼下垂，視力低下などを認める。眼窩・眼瞼発生例は横紋筋肉腫の中では特殊で，腫瘍の大きさや領域リンパ節転移の有無にかかわらず予後良好と考えられ，治療前病期分類は腫瘍の進展やリンパ節浸潤にかかわらずStage 1となる。治療方針は他の部位とは異なり，まずは生検にとどめ診断を確定し，Stage 1・Group Ⅲとして化学療法と放射線療法を行う。全摘可能であっても腫瘍を全摘出することは勧められていない。放射線照射も推奨されている。もし非切除治療後に局所再発した場合には，転移巣がコントロールできていれば眼球を含む眼窩内容の全摘出がIRSGでは推奨されている。

❸ 脳腫瘍

小児の脳腫瘍は小児がんの20％を占め固形腫瘍のなかでは最も頻度が高い。発生部位はテント上が60％，テント下が30％，脊髄が10％の比率である。組織型は多様性に富み，星細胞

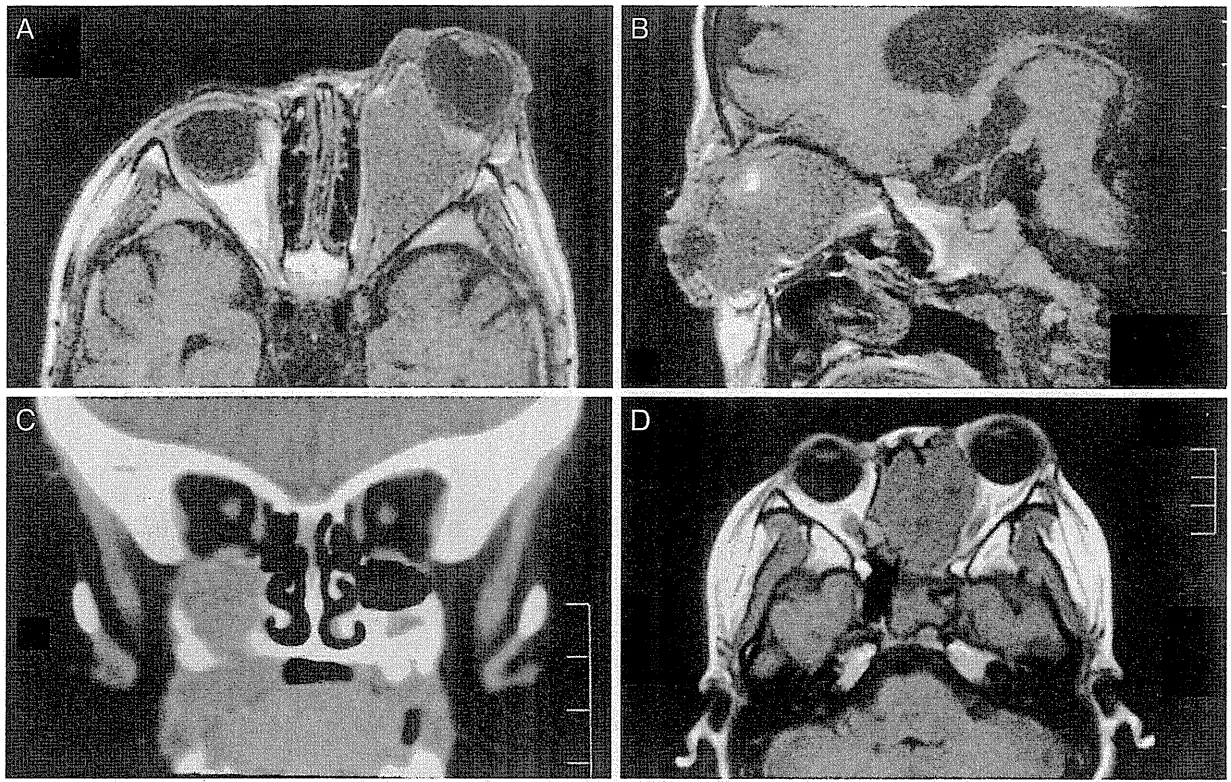

図2　眼窩内および眼窩外腫瘍

A：左眼窩内横紋筋肉腫(水平断)
右眼球が著明に前方に突出している。
B：左眼窩内横紋筋肉腫(矢状断)
眼球は前下方に突出し，腫瘍は眼窩上壁を上方に圧排している。
C：右上顎洞原発ランゲルハンス細胞組織球症
腫瘍は眼窩下壁と上顎洞下壁を破壊し突出している。
D：正中部篩骨洞原発横紋筋肉腫
眼球は左前方に突出し，腫瘍は眼窩内壁を破壊している。

腫・髄芽腫・胚細胞腫瘍・頭蓋咽頭腫・退形成星細胞腫・上衣腫などに分類される[5]。正中・傍正中部に多発し，髄液通過障害を起こしやすく水頭症を伴うことが多い。

症状は頭蓋内圧亢進や水頭症の症状としての，頭痛・不機嫌・嘔気・嘔吐・歩行障害・易転倒性・体重増加不良・発達障害・不器用・学業成績の不振・行動異常などが一般的であり，局在症状としてのけいれんや麻痺・運動障害・言語障害がみられる。脊髄腫瘍では筋力低下・膀胱直腸障害などがある。

眼科領域の症状も脳腫瘍には特徴的であり，眼球運動障害・眼位の異常・視力障害・視野障害などが発見の契機となることがある。脳腫瘍と診断したらうっ血乳頭の評価や視力・視野障害の評価が必須である。

治療は組織型と腫瘍の局在により大きく異なる。外科的に全摘出することが望ましいのは，小脳の pilocytic astrocytoma や頭蓋咽頭腫などの手術単独で治癒が期待できるものと，上衣腫などの化学療法や放射線療法の感受性が不良なものである。また，髄芽腫や primitive neuroectodermal tumor(PNET)などは外科切除単独では治癒が期待できないが，化学療法や放射線療法の感受性が高く併用療法が行われる。松果体部に発生する germinoma や胚細胞腫瘍は，化学療法や放射線療法の感受性が高く，腫瘍は生検にとどめることが一般的である。一方びま

ん性脳幹部神経膠腫は種々の治療に感受性が低く，一般的には手術適応とならず，有効な治療法が見出せていない。治療成績はいまだ満足のいくものではなく，小児がんの死亡原因の第1位を占めている。

④ 神経芽腫

神経芽腫は神経堤細胞を起源とし，副腎髄質や交感神経組織に発生し，カテコラミンを産生する腫瘍である[6]。小児がんの5～8％を占め，日本では年間100例程度の発生で，高リスク群は50例，中間リスク群は15例，低リスク群は30例程度と推測される。発症年齢は低年齢ほど多く，95％以上は10歳未満である。好発部位は副腎および後腹膜で，その他には後縦隔・頸部などにみられる。臨床症状は腹痛・嘔吐・胸痛・呼吸障害・四肢痛・発熱・貧血・紫斑・体重減少などである[7]。

診断と治療効果判定・経過観察に有用な腫瘍マーカーとして，カテコラミン代謝産物である尿中バニルマンデル酸（VMA）と尿中ホモバニリン酸（HVA）と血中NSEが有用である。

年齢（1歳6カ月以上は予後不良）・病期・病理組織分類・分子生物学的因子である*MYCN*増幅の有無が予後因子である。

治療は，低リスク群では外科療法が主となり，中間リスク群では外科＋化学療法が行われ，高リスク群では外科＋化学＋放射線療法による集学的治療を行う。高リスク群に対する日本での化学療法の代表はVCR＋CPA＋THP-adriamycin＋cisplatinによる05A3療法である。

期待生存率は，低リスク群は90％以上，中間リスク群は70％，高リスク群では30～40％である。日本では日本神経芽腫研究グループ（JNBSG）が2005年から多施設共同研究を行っている。

神経芽腫は眼科領域にも発生し，眼窩内や眼窩周囲の骨転移から腫瘍が伸展し，眼球突出を認めることがある。またopsoclonus myoclonus syndromeと呼ばれる眼球運動異常に小脳失調症状を合併する特徴的な合併症がみられることがある。また交感神経障害によるHorner症候群を認めることもある。眼窩内の腫瘍は外科切除や生検を行うことは一般的にはなく，腫瘍マーカーの値と他の部位の生検で診断を確定し，化学療法を行うことにより腫瘍の縮小を期待する。腫瘍が消失すれば放射線照射は行わない。

III. 眼窩内腫瘤性病変の鑑別

小児の眼窩内腫瘍を発見した時には，横紋筋肉腫，神経芽腫，網膜芽細胞腫，ユーイング肉腫，ランゲルハンス細胞組織球症，胚細胞性腫瘍，悪性リンパ腫などの悪性腫瘍の他にも，奇形腫や血管腫などを鑑別する必要がある。開創腫瘍生検による診断確定が望ましいが，眼窩内腫瘍単独の場合には生検の適応については慎重に検討する必要がある。腫瘍の局在部位によっては生検により視神経や外眼筋を損傷し視機能障害を引き起こす危険性や，あるいは骨破壊が必要となるなど安全な生検が困難な場合もある。

Neudorferらによる42例の2週から14歳の眼窩内腫瘍の小児例を対象とした報告では，22例は外科手術を行い病理所見で確定診断したが，20例は画像検査，臨床診断より経過観察とされている[8]。この報告では画像診断で血管腫18例・奇形腫16例・リンパ管腫5例・横紋筋肉腫2例・骨膜下膿瘍1例と診断した。未生検経過観察例では，平均経過観察期間38.2カ月で，すべての症例で経過は診断と一致しており，超音波検査が診断に有効であると結論している。我々も生検を行わず経過観察を行い自然消失した眼窩内腫瘍の1例を経験している（**図3**）。

眼窩内腫瘍を診断する際の各検査の特徴を挙げる。MRI検査は脂肪組織が明瞭に描出され，